J Mater Sci: Mater Med (2008) 19:3611–3619
DOI 10.1007/s10856-008-3508-0

Preparation and properties of a chitosan-based carrier of corneal endothelial cells

Xingshuang Gao · Wanshun Liu · Baoqin Han · Xiaojuan Wei · Chaozhong Yang

Received: 17 December 2007 / Accepted: 16 June 2008 / Published online: 19 July 2008

Abstract A novel chitosan-based membrane that was made of hydroxypropyl chitosan, gelatin and chondroitin sulfate was used as a carrier of corneal endothelial cells. The characteristics of the blend membrane, such as transparency, equilibrium water content, permeability, mechanical properties, protein absorption ability, hydrophilicity and surface morphology, were determined. To study the effects of the membrane on cell attachment and growth, rabbit corneal endothelial cells were cultured on this artificial membrane. The biodegradability and biocompatibility of the blend membrane were in vivo evaluated by its implantation into the muscle of the rats. Glucose permeation results demonstrated that the blend membrane had higher glucose permeability than natural human cornea. Scanning electron microscopy (SEM) analysis of the membranes demonstrated that no fibrils were observed. As a result, the optical transparency of the membrane was as good as the natural human cornea. The average value of tensile strength of the membrane was 13.71 MPa for dry membrane and 1.48 MPa for wet membrane. The value of elongation at break of the wet was 45.64%. The cultured rabbit corneal endothelial cells formed a monolayer on the blend membrane which demonstrated that the membrane was suitable for corneal endothelial cells to attach and grow. In addition, the membranes in vivo showed a good bioabsorption property. The mild symptoms of inflammation at sites of treatment could be resolved as the implant was absorbed by the host. The results of this study demonstrated that the hydroxypropyl chitosan-chondroitin sulfate-gelatin blend membrane can potentially be used as a carrier for corneal endothelial cell transplantation.

X. Gao · W. Liu (✉) · B. Han · X. Wei
College of Marine Life Sciences, Ocean University of China, Qingdao 266003, China
e-mail: WanshunLiu@hotmail.com

X. Gao
e-mail: xingshuanggao421@163.com

C. Yang
Dongfang Hospital of Ophthalmology, Qingdao 266021, China

1 Introduction

The corneal endothelium represents the most important part of the cornea. Only an intact endothelium with a sufficient cell density can function properly and maintain clarity of the cornea by its dehydrating pump function [1]. During life we experience a physiological reduction of corneal endothelial cell density of about 0.5% per year [2], which can not be compensated due to the limited proliferative capacity of these cells [3]. Furthermore, various conditions including Fuchs corneal endothelial dystrophy or increased intraocular pressure (IOP) after keratoplasty can also increase or accelerate irreversible endothelial cell loss [4, 5]. Until now it has only been possible to replace damaged endothelium by transplantation of a donor cornea [6, 7]. However, this treatment has several drawbacks, e.g., insufficient donor corneas, recurrent allograft rejection, and subsequent graft failure in certain cases.

With the development of tissue engineering and the methodological establishment of isolation and culture of corneal cells, it would be beneficial if cultured corneal endothelial cells could be transplanted for the treatment of diseases caused by corneal endothelial disorders. Some decades ago, scientists tried to manipulate endothelial cell density by transplantation of isolated cells using different

methods. Strategies to culture corneal endothelial cells onto biodegradable membranes were also their goal. So far, the carriers used for corneal endothelial cells included allograft cornea [8], thin gelatin membrane [9], hydrogel membrane [10], collagen matrix [11], collagen sheet [12], biodegradable polymers [13], amniotic membrane [14], Descemet membrane [15], and so on. These carriers had good biocompatibility. However, they hold some shortages, such as, immunological rejection, poor mechanical properties and uncontrolled degradation rate. These disadvantages have limited their clinical application. The present study aimed at searching for carrier materials that may have better cell attachment promoting properties and implantation applicability for corneal endothelial cells.

Chitosan (CTS) is a partially deacetylated derivative of chitin, being composed mainly of (1–4)-2-amino-2-deoxy-D-glucopyranose repeating units. It shows some interesting biological properties such as low immunogenicity [16], antibacterial property [17], mucoadhesivity [18], low cytotoxicity [19], biodegradability [20] and wound healing activity [21]. Therefore, it has been extensively used in tissue engineering. In addition, chitosan prompts the expression of extracellular matrix (ECM) protein in human osteoblasts and chondrocytes, and enhance the osteoblasts, fibroblast, keratinocyte and endothelium cell adhesion and proliferation [22]. It is capable of forming insoluble ionic complexes with the negatively charged glycosaminoglycan (GAGs) [23]. This ionic cross-linking mechanism can be used to immobilize chondroitin sulfates within hydrogel materials which mimic the GAG-rich ECM of the articular chondrocyte. Moreover, the biomembranes made of chitosan, collagen, chondroitin sulfate and hyaluronate have been used in reconstruction of cornea [24–26]. However, severe host inflammation in signs of fibrous encapsulation and corneal neovascularization were observed after the implantation of chitosan into cornea [27, 28]. In particular, the initially induced inflammation after scaffold implantation might endanger a successful engraftment of tissue-engineering constructs [29, 30]. Therefore, to be used as a carrier or scaffold material for corneal cells, their structure and composition must be modified to relieve the initial host tissue response after implantation.

In our previous study, to improve the biocompatibility of CTS, a water-soluble derivative of CTS- Hydroxypropyl chitosan (HPCTS) was prepared. We found out that this material was feasible to be applied to reconstruction of tissue engineered cornea [31]. Furthermore, we screened out a HPCTS-based blend membrane that was suitable for adhesion and growth of corneal epithelial cells. In this study, the preparation and properties of the blend membrane were described. At the same time, we studied the effects of the membrane on cell attachment and growth by culturing the rabbit corneal endothelial cells. In addition, the biodegradability and biocompatibility of the blend membrane were in vivo evaluated.

2 Materials and methods

2.1 Materials and regents

Wistar rats were purchased from Qingdao Laboratory Animal Center. HPCTS (degree of deacetylation = 75%, Mw = 35KD), chondroitin sulfate (Mw = 10KD) and biodegradable cross linker were prepared and purified by our lab. Gelatin, BSA and bFGF were purchased from Sigma Chemical Co. (USA). Materials for cell culture including Ham's F12 culture medium, DMEM culture medium fetal bovine serum (FBS) and penicillin-streptomycin (10,000 U/ml) in 0.85% saline were purchased from Gibco Co. (USA). Tissue culture flasks and 48-well plates were obtained from Corning Co. (USA). Lactate Dehydrogenase Kit was purchased from JianCheng Bioengineering Co. (Nanjing, China). All other reagents used were of reagent grade.

2.2 Preparation of HPCTS blend membrane

2% HPCTS solution was mixed with the 0.2% Cs aqueous solution and 2% Gel solution (weight ratio of HPCTS: Gel: Cs = 200:10:1) under agitation for 30 min at 40°C. Then, the solution was adjusted to pH10. A suitable amount of potassium acetate and cross linker was added to the mixture solution. The mixture was poured into a flat-bottomed glass dish of 20 cm in diameter, and then dried at 40°C for 24 h to form a thin membrane. The membrane was repeatedly washed with D-Hanks' balanced saline until the pH returned to a physiologic range to give the HPCTS-Gel-Cs blend membrane.

Membranes for in vitro cell culture and in vivo implantation studies were prepared under sterile conditions in a biosafety level II cabinet. All regents were either autoclaved or sterilized by filtering with 0.2 μm filters.

2.3 Measurement of the properties of the blend membrane

2.3.1 Transparency measurement

The transparency of the membrane pieces were examined by scanning them within the range of wavelengths (400–800 nm) using a TU-1800S UV-Visible Spectrophotometer (Beijing, China).

2.3.2 Measurement of equilibrium water content

The equilibrium water content of membrane was defined as the weight ratio of water content to the swollen membrane. Membranes were soaked in 0.1 M phosphate buffered saline (pH 7.4) for 24 h at room temperature. Then the membranes were removed from the buffer solution, placed between two pieces of dried filter paper to remove excess solution, and then weighed (W1). These samples were dried in a 110°C oven for 2 h, and weighed again to determine the dry weight (W2). The percentage of equilibrium water content (%) was calculated with the following equation:

$$\text{Equilibrium water content } (\%) = \frac{W1 - W2}{W1} \times 100\%. \quad (1)$$

2.3.3 Measurement of hydrophilicity

The hydrophilicity of the prepared membranes was evaluated by the sessile drop measurement of water contact angles using a contact angle/surface tension meter (Shanghai, China) at 25°C. The measurement was performed in three different points each sample.

2.3.4 Protein adsorption testing

The membranes with the area of 0.95 cm^2 were soaked into 4 ml 0.05%BSA solution, and kept at 37°C for 24 h. Then the membranes were taken out and the concentrations of the protein remnants in the solution were measured with the Coomassie brilliant blue method [32].

2.3.5 Determination of the mechanical properties

Samples were examined in both the dry and the swollen state. Before the start of test, the membranes were immersed into the PBS for 24 h. Membranes were gently placed on a rubber base and a sharp triple-blade tool was used to cut two rectangular specimens with 10.0 mm uniform width. The specimens were subsequently connected to the grips using mechanical clamps with rough surfaces to prevent slippage. The grips were part of an assembly designed to ensure that the initial length of the specimen between the clamp faces was 100 mm. Testing was performed at room temperature on an electron universal testing machine (Shenzhen, China) with 50 N capacity load cell. The specimens were subjected to uniaxial tension with an elongation rate of 10 mm/min. Testing continued until fracture of the specimen was achieved.

2.3.6 Permeability testing

Glucose permeability of the blend membranes was determined using a custom-made device. The blend membranes (1.5 cm in diameter) were placed into the apparatus without leaking. Then the apparatus was placed into an incubator at 37°C and 100 rpm. The glucose concentration of the solutions in each chamber was periodically measured with the DNS (3, 5-Dinitrosalicylic acid) method [33]. The permeability coefficient (P [cm/s]) of glucose was calculated from the rate of glucose concentrations change with time using the following equation [34]:

$$P = \frac{\frac{dc}{dt} \cdot V}{A \cdot C_0 \cdot 60} \quad (2)$$

where dc/dt stands for the increase of permeated cumulative glucose amount versus time (mg/min), V is the volume of the receiver compartment, A is the surface area of the membrane, C_0 is the initial glucose concentration in the donor compartment and 60 is the conversion factor from minute into second. The steady-state flux (dc/dt) was determined from the slope of the linear portion of cumulative permeated glucose amount versus time.

2.3.7 Surface characterization of the membrane

Membranes were fixed in a 2% glutaraldehyde solution, and dehydrated in a graded series of ethanol solutions. Afterwards, the membranes were dried in a Hitachi HCP-2 critical point dryer (Tokyo, Japan), sputter-coated with gold in a Hitachi HUS-5 GB high vacuum evaporator, attached to sample stubs and visualized using a Hitachi S-2400 scanning electron microscope (SEM).

2.4 Cell culture

Rabbit corneal endothelial cells were cultured in F12/DMEM (1:1) medium supplemented with 10% FBS. After reaching 80% confluence, the endothelial cells were rinsed twice with D-Hanks' balanced salt solution, incubated with a mixture of 0.25% trypsin and 0.01% EDTA at 37°C for 2 min, then neutralized with a culture medium containing 10% FBS. The cells at a density of 5×10^5 cells/cm^2 were cultured on 25 cm^2-plastic flasks in a CO_2 (5%) incubator at 37°C.

Sterile blend membranes (11 mm in diameter) were put in the wells of 48-well plates and the tissue culture polystyrene (TCPS) was used as a control substrate. The P2 cells were seeded onto the membranes at a density of 1×10^5 cells/cm^2. The cell/carrier constructs were cultured at 37°C/5% CO_2 with the medium changed every 3 days. Cell morphology and attachment were monitored using an image analysis system (Japan) connected to an Olympus IX70 inverted microscope (Japan).

The toxic effect of blend membranes on cells was quantitatively determined by measuring the lactate dehydrogenase (LDH) activities in the extracellular medium

released from damaged cells after 3d, 6d and 8d of culture, respectively. LDH activity was measured by using a LDH kit according to the protocol of the vendor. The optical density of the medium was read on a TU-1800S UV-Visible Spectrophotometer at the wavelength of 440 nm.

2.5 Evaluations of histocompatibility and degradability of membranes in vivo

The in vivo histocompatibility and degradability of membranes were examined by implanting the membranes into the skeletal muscle of Wistar rats. Female Wistar rats weighing about 200 g were kept under a specific pathogen free condition throughout the experiment. The sterile membranes (6 mm in diameter) were implanted into the skeletal muscle of anesthetized rats. The rats implanted with medical suture were set as controls. Three rats were sacrificed on 15d, 30d and 60d after the implantation, respectively. Membranes and their surrounding tissue were removed, and subsequently fixed in 4% neutrally buffered formaldehyde, embedded in paraffin, stained with haematoxylin–eosin (HE) and analyzed for histology.

The membranes retrieved on 30d postoperatively were processed for SEM examinations.

2.6 Statistical analysis

Data were expressed as means ± SD of a representative of three similar experiments. Statistical difference between treatment groups in the LDH release study was evaluated via one-way analysis of variance (ANOVA), and a value of $P < 0.05$ was considered significant (computed by SPSS version 10.0 Software).

3 Results

3.1 Optical transmittance of the blend membrane

Figure 1 summarized the light transmission through the samples in the light wavelength range (400–800 nm), which was measured as an indicator of membrane transparency. The light transmittance of samples exceeded 90% through the entire range of visible wavelengths. The results demonstrated that light transmission was close to the real cornea and met the quality criteria of corneal carrier.

3.2 The equilibrium water content and contact angle

The membrane used in this study had a fitting equilibrium water content of 71.3% which is close to that (78%) of the native corneal stroma. The contact angle of the membrane was 102.5°.

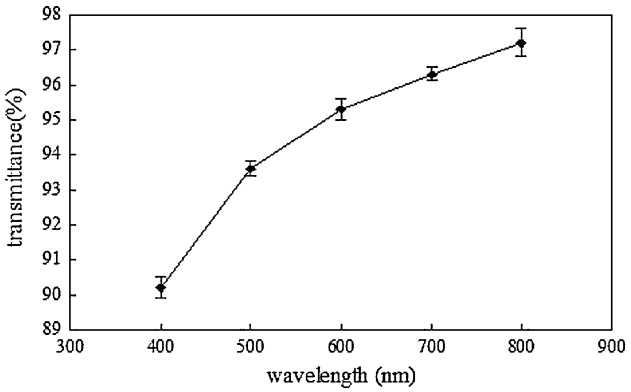

Fig. 1 Optical transmittance of the blend membrane, each point represents the mean ± SD of three experiments

3.3 Protein adsorption

The results of this study showed that the membrane held a protein adsorb capacity of 238 $\mu g \cdot cm^{-2}$. These results suggested that the artificial membrane had good protein adsorption ability. Simultaneously, the adsorbed proteins offered prerequisite for cell adhesion.

3.4 The permeability

The rate of glucose concentration changed with time was shown in Fig. 2. The glucose permeability of the blend membrane was 4.17×10^{-4} cm/s. This permeability was comparable with or even better than that of native cornea. Based on the published data, the permeability of native cornea was between 10^{-6} and 10^{-7} cm/s [35].

3.5 Mechanical properties

Mechanical properties of membranes, including tensile strength and elongation at break were measured. The average value of tensile strength was 13.71 MPa for dry

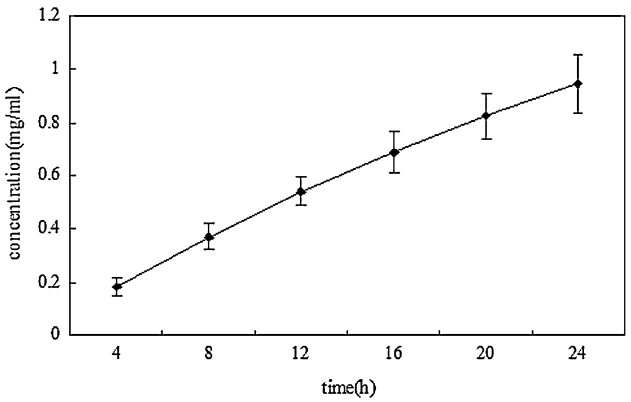

Fig. 2 The rate of glucose concentration change with time, each point represents the mean ± SD of three experiments

membrane and 1.48 MPa for wet membrane. Clearly, dry membrane had a higher strength and a higher rigidity than the membrane saturated with water. Moreover, the testing result sowed that the value of elongation at break was 45.64%. This result suggested that the membrane carried out a relatively high elongation at break.

3.6 Microstructural characteristics

The blend membrane, consisting of HPCTS, Gel and Cs, was fabricated by using a solvent casting/particulate leaching technique. Figure 3b showed the SEM image of a porous structure on the surface of the carrier. After salt was removed, the surface of the membrane possessed a porous structure. Figure 3 showed the comparison of the membrane surface before and after the potassium acetate treatment. The results demonstrated that the membrane performed a smoothly surface before adding potassium acetate to it (Fig. 3a). However, the roughness of the membrane surface was significantly increased with the addition of the poregen (data not seen).

3.7 Morphology and activity of the cells on the membrane

To investigate the morphology and activity of the cells on the membrane, we cultured the rabbit corneal endothelial cells on the membrane. Figure 5 showed the micrographs of rabbit corneal endothelial cells spread on the tested membrane surface and their spindle morphology. As a control, the same experiment was conducted on TCPS and the micrographic results were shown in Fig. 4. The results demonstrated that, within 24 h, the morphology of the cells changed from a rounded shape to a relatively extended shape. After the cells were cultured on the membranes for 2 days, a similar situation was observed on both tested membrane and TCPS in terms of cell adhesion and cell growth (Figs. 4a, 5a). However, compared with TCPS, the blend membranes performed an enhanced cell adhesion and cell growth after they were cultured for 3 days. At that time, the cells aligned themselves with elongated morphology and secreted extracellular matrix. On day 4, primary corneal endothelial cells reached confluence with a cobblestone appearance and cohesive organization. Furthermore, morphology changes were observed in all cases (Fig. 5b). Therefore, the results suggested that the tested blend membrane was more cytocompatible than TCPS for the growth of corneal endothelial cells. Over longer culture time, there was a trend that the cells proliferated faster on blend membrane than on TCPS (Figs. 4c, 5c).

As we know, LDH is a cytosolic enzyme released when cells are toxic or injured. To investigate the toxic effect of blend membranes on cells, we evaluated the LDH activity in the extracellular milieu. As shown in Fig. 6, LDH productions were significantly lower when the corneal endothelial cells were cultured on the blend membranes

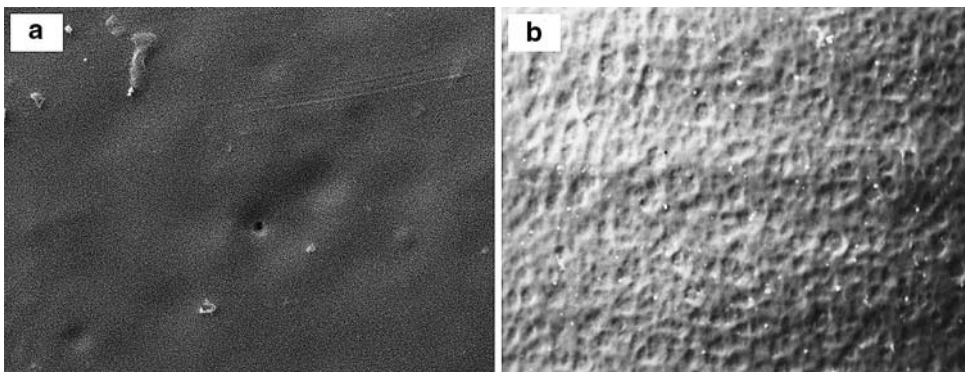

Fig. 3 SEM images on the surface of the blend membrane: (**a**) without poregen (1000×); (**b**) added potassium acetate as a poregen (1000×)

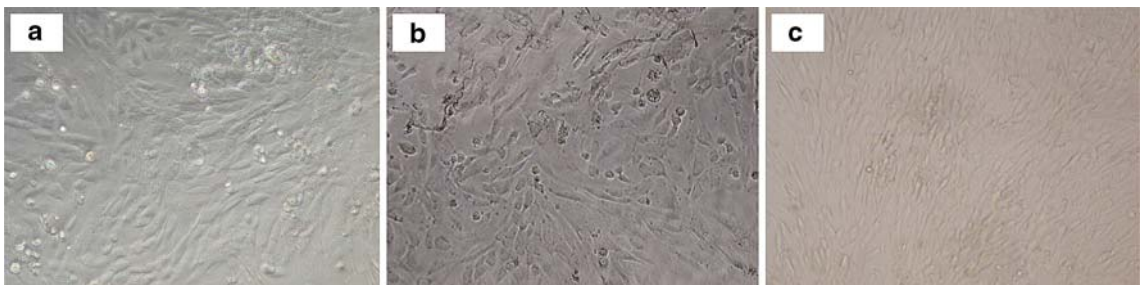

Fig. 4 The photomicrographs of rabbit corneal endothelial cells on TCPS after they were cultured for 2d (**a**), 4d (**b**) and 6d (**c**) (100×)

Fig. 5 The photomicrographs of rabbit corneal endothelial cells after 2d (**a**), 4d (**b**) and 6d (**c**) of culture on blend membranes (100×)

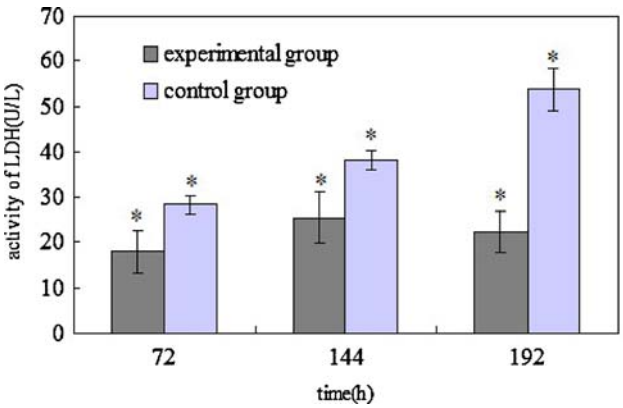

Fig. 6 LDH activity released to the culture medium from rabbit corneal endothelial cultured cells on blend membrane and TCPS after they were incubated for 3, 6 and 8 days. Each result represents the mean ± SD of three experimental data. Asterisk denotes significant differences of LDH release compared to the TCPS ($P < 0.05$) as determined by Student's *t*-test

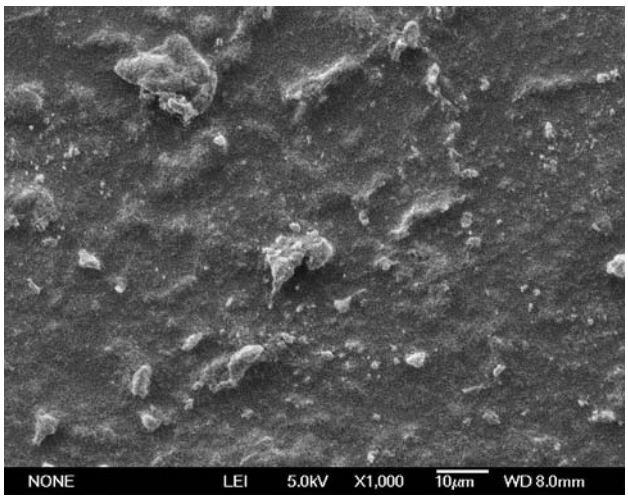

Fig. 7 SEM image on the surface of the membrane retrieved on 30-day postoperatively (1000×)

than they were cultured on the TCPS control ($P < 0.05$). The results demonstrated that the affinity of the blend membrane not only promoted the cell adhesion but also provided a better environment for cell growth.

3.8 Histocompatibility and biodegradability in vivo

No observable signs of inflammation, infection or distress were noticed in any of the animals implanted with the blend membranes for 2 months. However, post-mortem visual examination detected some inflammation in signs of implant encapsulation at the interface between the material and the host tissue in tested animals. On day 15, similar inflammations were observed in both the experimental group and the control group (Fig. 8a, b). On day 30, the implants in the experimental group showed an obvious degradation, and the encapsulation became thinner. In this period, the implants showed lack of vascular ingrowth (Figs. 7, 8c). In contrast, animals implanted with sutures displayed significant fibrous encapsulation surrounding the implanted area. On day 60, postoperatively, the membranes were totally degraded into fragments with a light inflammatory response around the implants and their surrounding area (Fig. 8d).

4 Discussion

Successful tissue engineering depends on the provision of a scaffold during the initial stages of reconstruction. In this study, we developed a novel chitosan-based blend membrane using solvent casting/particulate leaching technique. Utilization of a fused KAc mold in this method resulted in the formation of holes between pore walls in the carrier. Salt fusion treatment caused an increase in the compressive modulus of solvent cast scaffolds, possibly due to the formation of thick annular struts adjacent to holes in pore walls. The good transparency of the membrane satisfied the requirements for the carrier of corneal endothelial cells. Furthermore, the results demonstrated that three materials used for the synthesis of the membrane were compatible of, and formed a homopolymer that could increase the incidence of visible light. Among the materials, HPCTS was capable forming ionic complexes with the negatively charged Cs and Gel. This ionic cross-linking immobilized Cs and Gel within HPCTS material that functioned to mimic the ECM of the tissue.

The endothelium elicits net the ion transport outward from the stroma, which provides the driving force for fluid

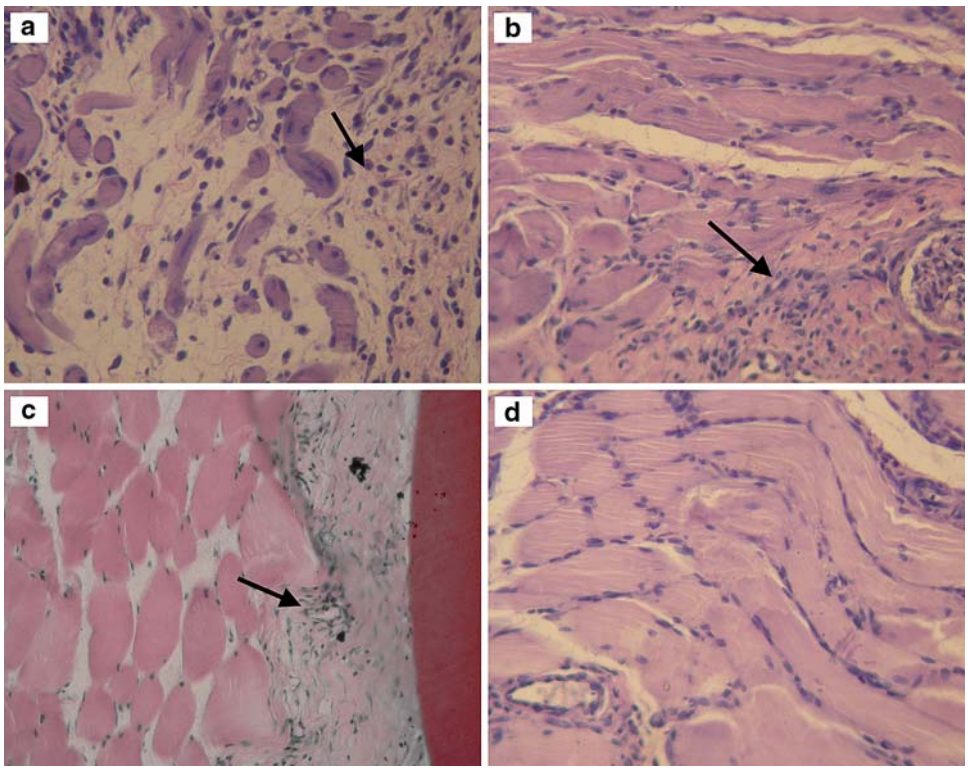

Fig. 8 Photomicrographs of the tissues implanted with: suture and retrieved on 15th day (**a**) and blend membranes (b. c. d.) and retrieved on 15th day (**b**), 30th day (**c**) and 60th day (**d**). The tissues were stained with HE (original magnification 200×). Note the inflammatory cells (arrows) surrounding the tissues in close vicinity to the implant. The inflammatory cells surrounding the tissues implanted with the blend membrane were almost disappeared on 60th day

transport into the tears and the anterior chamber [36]. For artificial cornea applications, some characteristics, such as vascularization, permeability to glucose and other small molecules has been suggested to be an important determinant to success as corneal tissue engineering scaffolds [37]. The good permeability of the membrane could ensure the nutrition in the aqueous fluid transfer into the stroma and epithelium tissue. Surface analysis results demonstrated that the good permeability of the blend membrane was the result of the formation of an open network with large KAc domains.

Hydrophilicity is one of the most important parameters affecting the biological response to an implanted material [38]. The water content of an artificial cornea was affected by several parameters, including the hydrophilicity, stiffness and pore structure of a matrix. The swelling extent was higher for the acetate treated blend membrane than the samples without poregen (data not seen). The comparison results suggested that the porous structure of the material might be the major factor that influences the extent of swelling of these samples. It was reported that moderate hydrophilicity promoted cell adhesion and proliferation. The moderate degree of wettability of the substrates allowed cells to deposit their own adhesion proteins and to exchange with adsorbed serum proteins more rapidly. The speed of this process was believed to be relatively slow on extremely hydrophobic or hydrophilic surfaces. This theory might explain why the cells did not adhere and proliferate properly on the extremely hydrophobic or hydrophilic surfaces [39]. The membranes used in this study had moderate wettability that closed to the native cornea. Thus they could provide a similar circumstance as native cornea in vitro.

Attachment, adhesion and spreading occur in the first phase of cell/material interactions. And these processes will influence the capacities of cell proliferation and cell differentiation when the cells contact with the artificial biomaterials. For in vitro cell culture, the adsorption of serum proteins by the growth substrate was considered the first step for the attachment of the actual cells. Therefore, protein adsorption played an important role in the attachment progress [40]. In addition, the cell adhesion process was steadily enhanced with the increasing amount of proteins attached on the material surface [41]. In this study, the high-quality protein adsorption ability of the membrane offered prerequisite for cell adhesion.

In this study the composition of the scaffold was designed to satisfy the requirements of cell growth and to promote the function of the cells. Our data demonstrated that corneal endothelial cells cultured on the membranes remained viable and maintained spindle morphology. Additionally, when the same number of corneal endothelial cells were seeded on the control TCPS, the cell growth was incomparable to that on the tested membrane (Figs. 4, 5). The CTS has been previously demonstrated as a biocompatible substrate for various types of cells [42–44]. Gelatin has been widely used in medicine due to its excellent

biocompatibility and biodegradability. Therefore, the observations that HPCTS promoted cell survival were expected in this study. In addition, as a kind of GAGs, chondroitin sulfate was pivotal in cell adhesion, migration, proliferation and differentiation [45].

The in vivo biocompatibility and degradability of the membrane were assessed in a rat model via the intramuscular implantation. It has been reported that when a biomaterial was implanted, the local tissue reacted initially to the injury, and then to the presence of the material. Inflammation is the most common reaction to all injury forms. And the inflammation normally leads to repair of the affected tissue. However, the abnormal wound healing can result in damage to the host tissue [46]. In the study, it was found that the degree in inflammatory reaction in surrounding tissue implanted with the membrane was less than medical suture counterparts observed on the 30^{th} day postoperatively (Fig. 8a–c). Additionally, it was found that the implantation of the membranes resulted in an acute inflammation reaction 2 weeks post implantation. The membranes were surrounded and encapsulated by fibrous connective tissue that was infiltrated by inflammatory cells after weeks of implantation. With the time went on, the membrane produced a lower degree of fibrous encapsulation formation. The most promising finding was that no obvious angiogenesis was observed during the experimental periods.

Besides their biocompatibility and other primary functions, medical implants were desired to show a good bioabsorption property. The persistence of biomaterials at a wound healing site might lead to chronic inflammation by the slowly degrading patches that elicited a long-term macrophage response [45]. The mild symptoms of inflammation at sites of treatment could be resolved as the implant was absorbed by the host. Hence, the fast bioabsorption rate of the blend membrane was another advantage for its potential uses in medical implants.

5 Conclusions

This study successfully combined the advantages of Gel, Cs and HPCTS via fabricating a highly porous blend membrane. The blend membrane was characterized by its good transparency, proper physical properties and degradability. The successful growth of the seeding cells on this membrane demonstrated the potential use of the membrane as a new biomaterial for tissue engineering. This study provided a starting point for the future development of chitosan-based scaffolds for tissue regeneration.

Further work in two directions is needed: (1) the mechanical strength and the suturability of the materials must be improved; (2) animal experiments are necessary to assess the utility of this cell-carrier constructs in vivo.

Acknowledgements This study is financially supported by the National High Technology Research and Development Program of China (863 Program, grant number: 2006AA02A132, 2007AA091603). The authors thank Professor Tang (American Red Cross) for critically reviewing this manuscript.

References

1. D.M. Maurice, J. Physiol. **221**, 43 (1972)
2. W.M. Bourne, H.E. Kaufman, Am. J. Ophthalmol. **81**, 319 (1976)
3. G.O. Waring, W.M. Bourne, H.F. Edelhauser, K.R. Kenyon, Ophthalmology **89**, 531 (1982)
4. M.M. Gagnon, H.M. Boisjoly, I. Brunette, M. Charest, M. Amyot, Cornea **16**, 314 (1997). doi:10.1097/00003226-199705000-00010
5. F. Bimbaum, T. Reinhard, D. Bohringer, R. Sundmacher, Arch. Clin. Exp. Ophthalmol. **243**, 57 (2005). doi:10.1007/s00417-004-0902-2
6. K.R. Dobbins, F.W. Price, W.E. Whitson, Cornea **19**, 813 (2000). doi:10.1097/00003226-200011000-00010
7. K. Engelmanna, J. Bednarzb, M. Valtink, Exp. Eye Res. **78**, 573 (2004). doi:10.1016/S0014-4835(03)00209-4
8. B. Aboalchamat, K. Engelmanna, M. Böhnke, P. Eggli, J. Bednarz, Exp. Eye Res. **69**, 547 (1999). doi:10.1006/exer.1999.0736
9. N. Lin, D.R. Meyer, J.P. Mcculley, Eye Sci. **4**, 156 (1989)
10. J. Mohay, T.M. Lange, J.B. Soltau, T.O. Wood, B.J. Mclaughlin, Cornea **13**, 173 (1994). doi:10.1097/00003226-199403000-00011
11. E.J. Orwin, A. Hubel, Tissue Eng. **6**, 307 (2000). doi:10.1089/107632700418038
12. T. Mimura, S. Yamagami, S. Yokoo, T. Usui, K. Tanaka, S. Hattori et al., Invest. Ophthalmol. Vis. Sci. **45**, 2992 (2004). doi:10.1167/iovs.03-1174
13. T. Hadlock, S. Singh, J.P. Vacanti, B.J. Mclaughlin, Tissue Eng. **5**, 187 (1999). doi:10.1089/ten.1999.5.187
14. Y. Fu, X.Q. Fan, W. Liu, Q.X. Shang, Chin. Ophthal. Res. **21**, 147 (2003)
15. K. Engelmanna, D. Drexler, M. Böhnke, Cornea **18**, 199 (1999). doi:10.1097/00003226-199903000-00010
16. P.K. Dutta, M.N.V. Ravikumar, J. Dutta, J. Macromol. Sci. **42**, 307 (2002)
17. Y.C. Chung, H.L. Wang, Y.M. Chen, Bioresour. Technol. **88**, 179 (2003). doi:10.1016/S0960-8524(03)00002-6
18. G. Borchard, H.L. Luegen, G.A. Deboer, J.C. Verhoef, C.M. Lehr, H.E. Junginger, J. Control. Release **39**, 131 (1996). doi:10.1016/0168-3659(95)00146-8
19. T. Mori, M. Okumura, M. Matsuura, K. Ueno, S. Tokura, Y.S. Minami et al., Biomaterials **18**, 947 (1997). doi:10.1016/S0142-9612(97)00017-3
20. S.H. Pangburn, P.V. Trescony, J. Heller, Biomaterials **3**, 105 (1982). doi:10.1016/0142-9612(82)90043-6
21. H. Ueno, H. Yamada, I. Tanaka, N. Kaba, M. Matsuura, M. Okamura, Biomaterials **20**, 1407 (1999). doi:10.1016/S0142-9612(99)00046-0
22. J.K.F. Suh, H.W.T. Matthew, Biomaterials **21**, 2589 (2000). doi:10.1016/S0142-9612(00)00126-5
23. V.F. Sechriest, Y.J. Miao, C. Niyibizi, A. Westerhausen-Larson, H.W. Matthew, C.H. Evans et al., J. Biomed. Mater. Res. **49**, 534 (2000). doi:10.1002/(SICI)1097-4636(20000315)49:4<534::AID-JBM12>3.0.CO;2-#
24. J. Chen, Q. Li, J. Xu, Y. Huang, Y. Ding, H. Deng, S. Zhao, R. Chen, Artif. Organs. **29**, 104 (2005). doi:10.1111/j.1525-1594.2005.29021.x
25. Y. Ding, J.T. Xu, J.S. Chen, C.Y. Wu, R. Chen, Recent Adv. Ophthalmol. **24**, 88 (2004)

26. Z.A. Yao, B.Q. Han, W.Z. Liu, W.S. Liu, High Technol. Lett. **14**, 95 (2004)
27. L.H. Chen, W.S. Liu, B.Q. Han, X.J. Wei, C.Z. Yang, Chem. Res. Chin. Univ. **28**, 880 (2006)
28. Y. Fu, P. Chen, X.Q. Fan, Chin. Ophthal. Res. **24**, 561 (2006)
29. H.J. Sung, C. Meredith, C. Johnson, Z.S. Galis, Biomaterials **25**, 5735 (2004). doi:10.1016/j.biomaterials.2004.01.066
30. M.W. Laschke, J.M. Haüfel, H. Thorlacius, M.D. Menger, J. Biomed. Mater. Res. **74**, 696 (2005). doi:10.1002/jbm.a.30371
31. X.S. Gao, W.S. Liu, B.Q. Han, Y. Liang, J. Ocean Univ. China **37**, 131 (2007)
32. M.M. Bradford, Anal. Biochem. **72**, 248 (1976). doi:10.1016/0003-2697(76)90527-3
33. G.L. Miller, Anal. Chem. **31**, 426 (1959). doi:10.1021/ac60147a030
34. R. Telse, K. Sigrid, Eur. J. Pharm. Biopharm. **58**, 137 (2004). doi:10.1016/j.ejpb.2004.03.010
35. B.E. McCarey, F.H. Schmidt, Curr. Eye Res. **9**, 1025 (1990). doi:10.3109/02713689008997577
36. M. Stefan, P. Uwe, Prog. Retin. Eye Res. **26**, 359 (2007). doi:10.1016/j.preteyeres.2007.02.001
37. T.V. Chirila, Biomaterials **22**, 3311 (2001). doi:10.1016/S0142-9612(01)00168-5
38. C.X. Li, A. Christopher, Siedlecki, Biomaterials **28**, 3273 (2007). doi:10.1016/j.biomaterials.2007.03.032
39. P.B.V. Wachem, A.H. Hoget, T. Beugeling, J. Feijen, A. Bantjes, J.P. Detmers et al., Biomaterials **8**, 323 (1987). doi:10.1016/0142-9612(87)90001-9
40. M.M. Browne, G.V. Lubarsky, M.R. Davidson, R.H. Bradley, Surf. Sci. **553**, 155 (2004). doi:10.1016/j.susc.2004.01.046
41. T. Yokota, T. Terai, T. Kobayashi, T. Meguro, M. Iwaki, Surf. Coat. Tech. **201**, 8048 (2007). doi:10.1016/j.surfcoat.2006.03.051
42. H. Ueno, M. Murakami, M. Okumura, T. Kadosawa, T. Uede, T. Fujinaga, Biomaterials **22**, 1667 (2001). doi:10.1016/S0142-9612(00)00328-8
43. M. Risbud, M. Bhonde, R. Bhonde, Cell Transplant. **10**, 195 (2001)
44. J.M. Chupa, A.M. Foster, S.R. Sumner, S.V. Madihally, H.W.T. Matthew, Biomaterials **21**, 2315 (2000). doi:10.1016/S0142-9612(00)00158-7
45. Y.L. Chen, H.P. Lee, H.Y. Chan, L.Y. Sung, H.C. Chen, Y.C. Hu, Biomaterials **28**, 2294 (2007). doi:10.1016/j.biomaterials.2007.01.027
46. S. Vijayasekaran, J.H. Fitton, C.R. Hicks, T.V. Chirila, G.J. Crawford, I.J. Constable, Biomaterials **19**, 2255 (1998). doi:10.1016/S0142-9612(98)00128-8